Title: Purkinje Cell Activity in Medial and Lateral Cerebellum During Suppression of Voluntary Eye Movements in Rhesus Macaques

Abbreviated title: Cerebellar activity during antisaccades

Eric Avila[1,2#], Nico A. Flierman[1,2#], Peter J. Holland[3], Pieter R. Roelfsema[1,4,5], Maarten A. Frens[2], Aleksandra Badura[1,2*] and Chris I. De Zeeuw[1,2*]

[1] Netherlands Institute for Neuroscience, Amsterdam, 1105 BA, The Netherlands

[2] Department of Neuroscience, Erasmus MC, Rotterdam, 3015 CN, The Netherlands

[3] School of Psychology, University of Birmingham, Birmingham, B15 2TT, UK

[4] Department of Integrative Neurophysiology, VU University, Amsterdam, 1081 HV, The Netherlands

[5] Department of Psychiatry, Academic Medical Centre, Amsterdam, 1105 AZ, The Netherlands

[#] These authors contributed equally to this work.

EA current address: Center for Neural Science, New York University, New York, 10003, USA.

[*]**Correspondence**:

Aleksandra Badura (a.badura@erasmusmc.nl)

Department of Neuroscience, Erasmus MC

Wytemaweg 80, 3015 CN Rotterdam

tel: 0031-(0)10 7043589

Chris I De Zeeuw (c.de.zeeuw@nin.knaw.nl)

Netherlands Institute for Neuroscience

Meibergdreef 47,1105 BA, Amsterdam

tel: 0031-(0)20- 5665500

Number of pages: 40

Number of figures: 5

Abstract: 246 words.

Introduction: 626 words.

Discussion: 1440 words.

Competing interests

The authors declare no competing interests.

Acknowledgements

We thank Kor Brandsma and Anneke Ditewig for their excellent biotechnical assistance; Beerend Winkelman for providing the MATLAB code for spike sorting; Chris van der Togt for providing assistance with stimulus presentation; Mario Negrello for providing the MATLAB code for saccade detection; Geert Springeling, Peter Thier, Peter W. Dicke, Ruud Smith for their help with anatomical scans and 3D model building; and Kaushik J. Lakshminarasimhan for helpful comments in the analysis. This research was supported by FP7-C7 European Commission, the Marie Curie Initial Training Network ITN-GA-2009-238214, ENW-Klein, ZonMw (VIDI/917.18.380,2018), Netherlands Organization for Scientific Research, European Research Council (Advanced Grant and Proof of Concept Grant), Medical NeuroDelta Programme, Topsector Life Sciences & Health (Innovative Neurotechnology for Society or INTENSE), and the Albinism Vriendenfonds Netherlands Institute for Neuroscience.

Abstract

Consciously suppressing responses to distracting external stimuli helps us to reach our goals. This volitional inhibition of a specific behavior is supposed to be mainly mediated by the cerebral cortex; however recent evidence supports the involvement of the cerebellum in this process. It is currently not known whether different parts of the cerebellar cortex play differential or synergistic roles in planning and execution of this behavior. Here, we measured Purkinje cell (PC) responses in the medial and lateral cerebellum in two rhesus macaques during the antisaccade task. In this task the non-human primates were instructed to make a saccadic eye movement away from a target, rather than towards it. Our data shows that the cerebellum plays an important role not only during execution of the antisaccades, but also during the volitional inhibition of eye movements towards the target. Simple Spike (SS) modulation during the instruction and execution period of pro- and antisaccades is prominent in PCs of both medial and lateral cerebellum. However, only the SS activity in the lateral cerebellar cortex contains information about trial identity and shows a stronger reciprocal interaction with complex spikes. Moreover, SS activity of different PC groups modulate bidirectionally in both regions, but the PCs that show facilitating and suppressive activity are predominantly associated with instruction and execution, respectively. These findings show that different cerebellar regions and PC groups contribute to goal-directed behavior and volitional inhibition, but with different propensities, highlighting the rich repertoire of cerebellar control in executive functions.

Keywords: Flexible behavior, simple spikes, complex spikes, executive control, antisaccade, non-human primates

Significance Statement

The antisaccade task is commonly used in research and clinical evaluation as a test of conscious and flexible control of behavior. It requires volitional suppression of prosaccades, a function that has been attributed to the neocortex. However, recent findings indicate that cerebellum also contributes to this behavior. We recorded from neurons in the medial and lateral cerebellum to evaluate their responses in this task. We found that both regions significantly modulated their activity during this task, but only cells in the lateral cerebellum encoded the stimulus identity in each trial. These results indicate that the cerebellum actively contributes to the control of flexible behavior and that lateral and medial cerebellum play different roles during volitional eye movements.

Introduction

In a dynamic environment, volitional control of behavior is necessary to make flexible, well-adapted choices. This often requires selective suppression of responses to external stimuli, a hallmark of conscious, executive control (Diamond, 2013). In a laboratory setting, we can measure this complex behavior using the antisaccade task. It requires the subjects to refrain from looking at a suddenly appearing target and instead execute a saccade to the (unmarked) mirror position of that target (Everling and Fischer, 1998; Mitchell et al., 2002; Munoz and Everling, 2004). Similar to other volitional movements, many regions in the cerebral cortex have been identified as crucial for the correct execution of the antisaccade task (Funahashi et al., 1993; Schlag-Rey et al., 1997; Gottlieb and Goldberg, 1999; Bunge et al., 2005; Hakvoort Schwerdtfeger et al., 2012; Everling and Johnston, 2013; Cutsuridis et al., 2014). Given its reciprocal connections with the relevant neocortical regions (Kelly and Strick, 2003), the cerebellum may form an additional hub in this voluntary motor control circuitry (Tanaka et al., 2003; Peterburs et al., 2012; Brunamonti et al., 2014; Kunimatsu et al., 2016; Dacre et al., 2019). This possibility is corroborated by recent findings that the cerebellum participates in movement planning (Ashmore and Sommer, 2013; Giovannucci et al., 2017; Deverett et al., 2018; Gao et al., 2018; Kostadinov et al., 2019). However, to what extent different parts of the cerebellum contribute to the planning and execution of the antisaccades, and complex movements in general, is unclear (Miall et al., 1993; Thach, 2007; Ito, 2008; Gao et al., 2018, 2019; Chabrol et al., 2019; De Schutter, 2019).

Several studies have indicated that execution of simple or reflexive movements may be controlled by Purkinje cells (PCs) in the medial part of the cerebellum, whereas complex

118 behaviors, which require instruction, inhibition and planning, might be controlled by more lateral
119 parts (Strick et al., 2009; Caligiore et al., 2017; Chabrol et al., 2019; De Schutter, 2019;
120 Sendhilnathan et al., 2020). Others however, advocate that both simple and complex movements
121 can be controlled by the same group of PCs (Gao et al., 2018, 2019), the location of which in the
122 cerebellar cortex may be determined by the PC-to-effector pathway (Voogd et al., 2012). Settling
123 these questions would require monitoring of spiking activity of PCs in both medial and lateral
124 cerebellar areas during a motor task that includes the execution of both simple and complex forms
125 of movements related to the same effector.

126 Here, we investigated the hypotheses that (1) PCs in the cerebellum play a role in the
127 volitional inhibition of stimulus-driven eye movements during the antisaccade task; and (2) that
128 PCs in medial and lateral cerebellum differentially contribute to pro- and antisaccades. More
129 specifically, we set out to study modulation of randomly selected saccade-related PCs in the medial
130 (oculomotor vermis, OMV) and lateral (crus-I/II) cerebellum of non-human primates (macaca
131 mulatta) during the generation of both pro- and antisaccades (**Fig. 1**). We found that Simple Spike
132 (SS) modulation during the instruction and execution periods of pro- and antisaccade trials was
133 prominent in PCs in both cerebellar regions. However, whereas SS activity in the lateral
134 cerebellum contained information about the trial identity, we were not able to detect this in the
135 vermis. In addition, Complex Spike (CS) activity showed a higher level of reciprocity with respect
136 to SS activity in the lateral cerebellum. Although the PC activity modulated bidirectionally in both
137 cerebellar regions, the PCs in the lateral cerebellum that facilitated their activity, so called upbound
138 PCs (De Zeeuw, 2021), contributed most prominently to the instruction of antisaccade trials.
139 Together, our data are adding to the growing body of evidence for a role of the cerebellum in

140 executive control and are inciting the field to explore cerebellar activity under conditions where
141 response inhibition is engaged.

142

143 **Materials and Methods**

144 *Animals*

145 All procedures complied with the NIH Guide for the Care and Use of Laboratory Animals
146 (National Institutes of Health, Bethesda, Maryland), and were approved by the institutional animal
147 care and use committee of the Royal Netherlands Academy of Arts and Sciences
148 (AVD8010020184587). Two adult male non-human primates (NHPs, Macaca mulatta), Mi and
149 Mo, were used in this study.

150 *Surgical procedures*

151 Animals were prepared for eye movement and awake, extracellular single unit recordings
152 in the cerebellum using surgical and electrophysiological techniques in a two-step procedure
153 (Roelfsema et al., 2012). Under general anesthesia induced with ketamine (15 mg/kg, i.m.) and
154 maintained under intubation by ventilating with a mixture of 70% N2O and 30% O2, supplemented
155 with 0.8% isoflurane, fentanyl (0.005 mg/kg, i.v.), and midazolam (0.5 mg/kg • h, i.v.), we first
156 implanted a titanium head holder to painlessly immobilize the NHP's head. Four months later,
157 once the NHPs had mastered the behavioral task (see below), a custom-made 40 mm chamber was
158 implanted under the same anesthesia conditions as described above to gain access to the cerebellum
159 with a 25 angle (**Fig. 1B**). Animals recovered for at least 21 days before training was resumed.

160 *Behavioral task*

161 Animals were trained to perform a randomized interleaving pro- and antisaccade task in 8
162 different directions (cardinal and diagonal directions), with amplitudes between 5˚ and 14˚ (**Fig.**
163 **1A**). All recordings were conducted in complete darkness. During training and experiments, NHPs
164 were seated in a primate chair (Crist Instrument, USA) with their head restrained at 100 cm from
165 a screen with a resolution of 1,024 x 768 pixels. Visual stimuli were presented by a CRT-Projector
166 Marquee 9500 LC (VDC Display Systems, Florida, USA) with a refresh rate of 100 Hz. Binocular
167 vision was unrestricted. A trial started when the animal fixated on a red or green fixation point at
168 the center of the screen for a random time between 300-500 ms. Next, a red target appeared in one
169 of 8 different target locations. After 100 ms the fixation point changed to gray and the NHP was
170 allowed to perform either a prosaccade toward the target (when fixation point was red) or
171 antisaccade in the opposite direction with the same amplitude as the target, (when fixation point
172 was green) within 500 ms (in the figures colors of fixation point and target were changed to blue
173 and magenta to accommodate colorblind readers). The animals received liquid reward if they
174 performed a correct saccade (within 6˚ of the (anti-)target) and maintained fixation for 100 ms.
175 Within a single block the 8 (targets) * 2 (pro/anti) possible configurations were presented in a
176 random order.

177 *Recordings*

178 Position of the right eye was recorded with an infrared video-based eye tracker (iViewX
179 Hi-Speed Primate, SMI GmbH, Germany) at a sampling rate of 350 Hz. The eye tracker was
180 calibrated before every recording session by having the animal look at 1˚ target grid consisting of
181 9 points (one at the center of the screen and 8 points 10˚ apart) to adjust the offset of X and Y
182 position by hand. Pre and post-surgical MRI-images were used to build a 3D model of the skull
183 and cerebellum for anatomical localization of cerebellar oculomotor vermis (lobules VI and VII)

184 and lateral cerebellum (crus I/II; **Fig. 1B** (Sendhilnathan et al., 2020). Single-unit recordings were
185 obtained using tungsten glass-coated electrodes (1-2 MΩ, Alpha Omega Engineering, Nazareth,
186 Israel) through a 23-gauge guide tube, which was inserted only through the dura. A motorized
187 microdriver (Alpha Omega Engineering, Nazareth, Israel) with a 1-mm spaced grid was used to
188 introduce the electrode and map the recording sites with a maximum resolution of 0.25 mm.

189 *Data Analysis Software*

190 All analyses were performed off-line using custom scripts written in MATLAB
191 (Mathworks, Natick, MA, USA).

192 *Eye movement analysis*

193 Eye position was sampled at 350 Hz with an infrared video eye tracker which tracked the
194 pupil center of mass. Noise was reduced using a finite impulse response filter and a savitzky-golay
195 filter (20 ms window). Eye velocity and acceleration traces were created by differentiating the
196 signal. Eye acceleration was further processed using a median filter. Saccade onset and offset were
197 detected using an adaptive threshold based on 6 s.d. of the noise during fixation from the recording
198 session of that day as described in Nyström and Holmqvist (2010) (Sendhilnathan et al., 2020).
199 Trials with reaction times less than 80 ms were excluded, as these were thought to represent
200 anticipatory actions.

201 *Electrophysiological analysis and statistics: Simple spikes (SSs)*

202 To perform statistical analysis, neurons were required to have at least 5 recorded trials per
203 direction as well as per pro- or antisaccadic condition. Only neurons with significant saccade-
204 related SS activity and only correct trials were incorporated in the analyses. The latter choice was
205 based on the fact that both NHPs Mo and Mi exhibited an expert level performance reaching >90%

206 correct responses, rendering insufficient statistical power to analyze the incorrect trials. A neuron
207 was considered to be saccade-related when SS firing during the baseline period (defined as the
208 window 400 to 50 ms before trial onset in the intertrial interval), was significantly different from
209 the saccade execution period activity (defined as the 150 ms time-window after saccade onset) for
210 at least one of the 8 directions (Wilcoxon rank test; $p < 0.05$). We then computed the instantaneous
211 SS firing rate of the neurons using a continuous spike density function (SDF) generated by
212 convolving the spike train with a Gaussian function of $\sigma = 50$ ms width and averaging all the
213 individual spike density functions (Sendhilnathan et al., 2020). We compared the number of spikes
214 for all pro- and antisaccade trials of each PC using a Kolmogorov-Smirnov test, and subsequently
215 determined whether the activity of a PC was significantly different between a pro- and antisaccade
216 with a p value < 0.05. The characteristics of the saccade-related activity, as previously reported in
217 PC recordings, was quite heterogeneous. On that account, we categorized the PC activity as
218 *facilitation*, if the activity increased after instruction or saccade onset, or as *suppression,* if the
219 activity decreased. For the instruction period, we compared the mean firing rate of each cell from
220 a window 400 ms before instruction onset to a period of 300 ms at the end of the instruction period.
221 For the saccade period we compared the mean firing rate of each cell from a window of 150 ms
222 before saccade onset to a window from saccade onset to 150 ms after saccade onset (Wilcoxon
223 signed rank, p value of < 0.05).

224 To determine the correlation between kinematic parameters and neuronal activity we
225 determined Pearson's correlation coefficient (r) for all neurons in the two tasks. Modulation ratios
226 for both areas were obtained by computing the ratio between the response during pro- and
227 antisaccades.

228 Changes in firing rate during the instruction period were computed by taking the
229 differences between the mean firing rates during the baseline period separately for pro- and
230 antisaccade trials. For the saccade period, we compared the mean activity 150 ms before the
231 saccade onset to a period 150 ms after saccade onset.

232 We performed a demixed principal component analysis as described by Kobak et al. (2016)
233 to decompose the population activity into individual components and extract the dependence of
234 the PCs on the two stimulus conditions. The dPCA data analysis tool code is available at
235 http://github.com/machenslab/dPCA (Kobak et al., 2016). Furthermore, all standard settings were
236 used; data were aligned to instruction offset and binned in 100 ms bins. For determining cross-
237 validated classification accuracies a 100 iterations were used.

238 *Electrophysiological analysis and statistics: Complex spikes (CSs)*

239 Cells were included into the analysis for complex spikes if they had a CS firing rate of
240 between 0.5 and 2 hz over the entire recording session and at least 5 trials for every of the 8 pro-
241 and antisaccade directions. To determine if the CS modulated to one of the task epochs, we
242 determined whether the CS rate significantly exceeded baseline levels during either the instruction
243 or the saccade window (50 - 350 ms after onset of the instruction and -150 to +150 ms around the
244 onset of the saccade). Baseline firing was calculated for a period of 500 ms of inter-trial activity,
245 and the modulation was considered significant if firing rate exceeded ± 3 standard deviations from
246 baseline.

247 Reciprocity of modulation between SS and CS rates was determined by finding the peak
248 of the modulation of CS and SS responses during the same 300 ms windows (50 - 350 ms after
249 instruction onset or -150 - 150 ms around the saccades). We first calculated the peak firing rate

250 changes for SS and CS from baseline (ΔCS, ΔSS), and next determined the SS-CS interaction, i.e.
251 reciprocity (ΔCS*ΔSS). Subsequently, we used a linear regression model to find out whether there
252 was an association between reciprocity in the instruction period and reciprocity during the saccade
253 period.

254 **Results**

255 *Pro- and antisaccades and related PC activity in medial and lateral cerebellum*

256 We trained two adult, male rhesus macaques (referred to as NHPs Mo and Mi) to perform
257 a randomized, interleaved pro- and antisaccade task. In the prosaccade trials, the NHPs performed
258 a (pro) saccade to a single visual target in one out of eight different locations separated 45˚ from
259 each other. Instead, in antisaccade trials, the NHPs were trained to suppress the prepotent saccade
260 to a visible target and perform a saccadic eye movement in the opposite direction to an unmarked,
261 mirror position (**Fig. 1A**).

262 A trial started with the appearance of the central fixation point (instruction period), the
263 color of which determined the trial condition. The colors red and green were the instruction cues
264 for prosaccade and antisaccade movements, respectively (these colors are presented as magenta
265 and blue in the figures to accommodate color-blind readers). Following the instruction period (300-
266 500 ms), a target appeared randomly at one of the eight different locations, while NHPs maintained
267 fixation on the central point. After 100 ms the central fixation point turned gray, serving as the
268 "go-cue". Animals had 500 ms to execute the pro- or antisaccade eye movement (saccade period)
269 before the trial was aborted. This task design temporally separates the initial neural representation
270 of the stimulus (300-500 ms long instruction period) from the subsequent movement execution
271 (saccade period) (Amador et al., 1998).

272 Following the training period, we performed single-unit electrophysiological recordings.
273 We recorded randomly from 90 PCs in medial and 72 PCs in lateral (Crus-I/II) cerebellum during
274 122 behavioral sessions (**Fig. 1B**). We removed trials with reaction times shorter than 100 ms
275 following the "go-cue" to avoid contamination with data from "anticipatory" saccades; these
276 reflect a visual, involuntary reflex towards a novel stimulus in the environment and do not
277 represent correctly planned saccades (Goldring and Fischer, 1997; Coe and Munoz, 2017). We
278 only considered correct trials for further analysis, as we did not have enough power to analyze
279 error trials due to the high performance of both NHPs (94.1 ± 5.6% and 94.4 ± 5.3% for Mo and
280 Mi, respectively). Eye movements during antisaccades exhibited longer reaction times, lower peak
281 velocities, larger amplitudes, and longer durations than prosaccades (**Fig. 1C**).

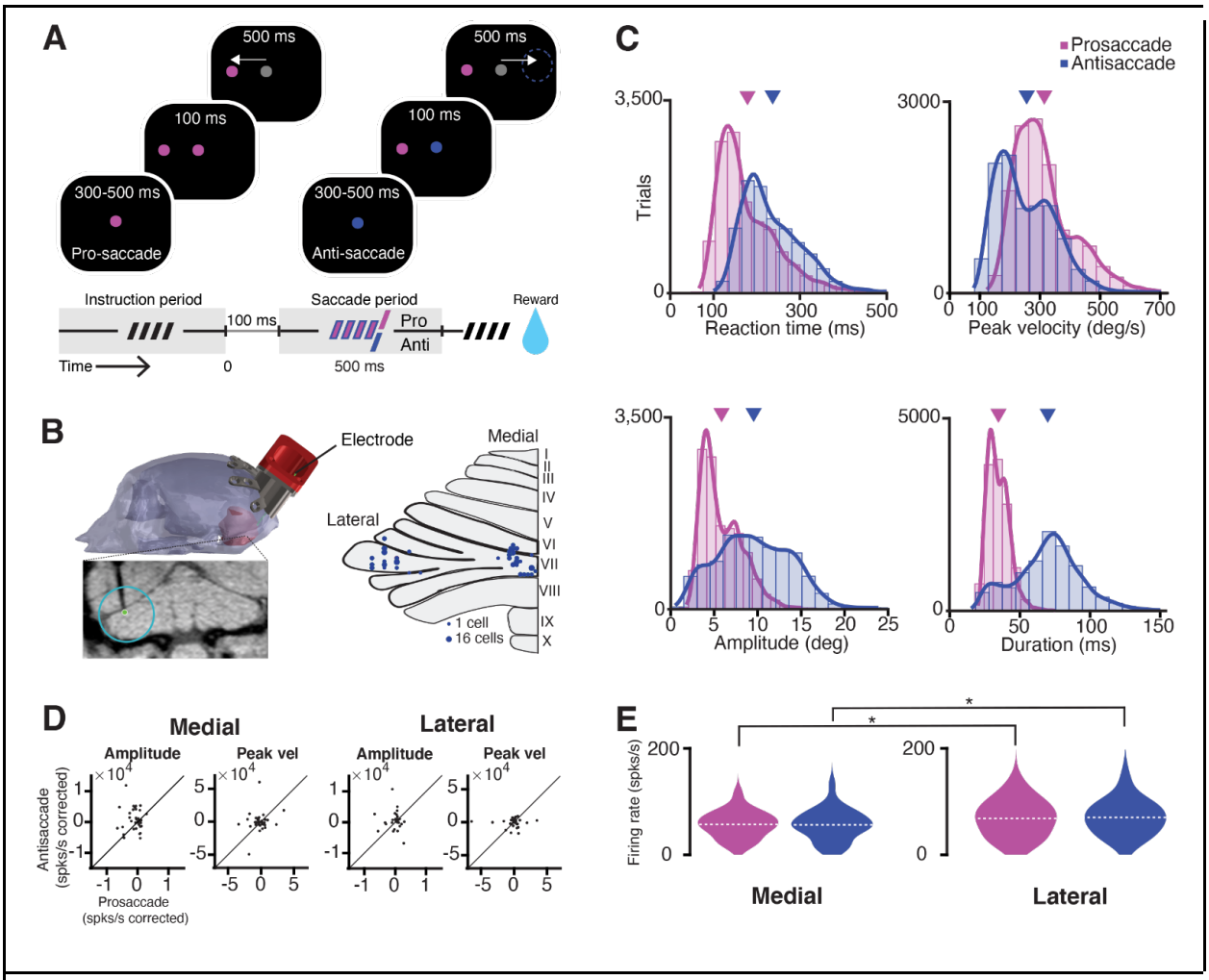

Figure 1. Task, recording location, saccade kinematics and related PC firing characteristics. ***A***, A scheme representing the different periods of the task. Trial condition was indicated by the color of the fixation point. After a random delay between 300-500 ms (i.e., instruction period, dashed symbol) a target appeared in one of 8 locations, while NHPs were required to maintain fixation for 100 ms. Next, the fixation target switched to gray, and NHPs were given 500 ms to execute a saccade (i.e., saccade period) towards the target (prosaccade) or the mirror position of the target (antisaccade). ***B***, ***left,*** CT-based 3D-reconstruction of the skull of Mi; ***bottom***, coronal MRI section showing the localization of an electrode in the left lateral cerebellum; ***right***, overview of the localization of recordings sites in the medial (vermal lobules VIc and VII) and lateral cerebellum (crus-I/II, left hemisphere). ***C***, Features of kinematics of all prosaccades (magenta; monkey Mo n = 6114, monkey Mi n = 6670) and antisaccades (blue; Mo n = 4114, Mi n = 6305) for all trials over the 122 recording sessions. Antisaccades were characterized by longer reaction times (pro- mean 178.4 ms ± 70.6 s.d.; anti- mean 236.6 ms ± 72.7 s.d.; $p < 0.0001$), lower peak velocities (pro- mean 311.8˚/s ± 102.6 s.d.; anti- mean 253.4˚/s ± 103.1 s.d.; $p < 0.0001$), bigger amplitudes (pro- mean 5.8˚ ± 2.3 s.d.; anti- mean 9.5˚ ± 4.1 s.d.; $p < 0.0001$), and longer durations (pro- mean 34.7 ms ± 7.9 s.d.; anti- mean 69.8 ms ± 24 s.d.; $p < 0.0001$). Triangles in magenta and purple indicate means of pro- and antisaccade movement parameters, respectively. ***D***, Scatter plots with corrected PC activity after a linear regression model fitted to amplitude or peak velocity during all pro- and antisaccades in medial (left) and lateral (right) cerebellum. ***E***, Violin plots showing the mean average simple spike firing rate for all cells during prosaccades (magenta) and antisaccades (blue) for medial (left) and lateral (right) cerebellum). Dashed lines depict the mean value for the population. The asterisks

show significance levels for a Wilcoxon rank sum test for the comparison between medial and lateral cerebellum in each condition (pro medial vs. lateral $p = 0.04$; anti medial vs. lateral $p = 0.03$).

A neuron was considered to be saccade-related if SS activity during the beginning of the saccade period (i.e., from saccade onset to 150 ms after saccade onset) was significantly different from the intertrial interval period (see **Methods**). Approximately half of the cells recorded in both areas fulfilled this criterion (n = 40 (44%) for the medial, and n = 38 (53%) for the lateral cerebellum). All subsequent analyses were performed only for these cells unless noted otherwise (n = 78 PCs). The average number of trials per cell in the medial cerebellum was 75 ± 49 and 71 ± 47 for pro- and antisaccades, respectively, while in the lateral cerebellum these numbers were 80 ± 52 and 76 ± 50, respectively.

To assess whether there was a correlation between saccade parameters and PC SS firing rate, we regressed the firing rates in the two recording areas to amplitude or peak velocity and compared the corrected firing rate using the regression coefficient (ß) between pro- and antisaccade (corrected firing = firing rate/regression coefficient). We found no significant correlations between SS firing rate and saccade amplitude or saccade peak velocity in neither the medial nor the lateral cerebellum (**Fig. 1D**). This allowed us to directly compare pro- and antisaccade trials between the two areas by pooling the mean firing rates of each cell in each condition. SS activity during saccade execution was significantly higher in the lateral cerebellum compared to that in the medial cerebellum for both pro- and antisaccade trials (mean and s.d., medial pro 66.7 ± 30 spks/s vs. lateral pro 69.3 ± 39 spks/s, $p = 0.04$; medial anti 68 ± 36 spks/s vs. lateral anti 71.8 ± 39 spks/s, $p = 0.03$; Wilcoxon rank sum test) (**Fig. 1E**).

303 *PCs in both medial and lateral cerebellum modulate their activity during the task but with different*
304 *characteristics*

305 The activity profile of the PCs followed roughly one of two patterns, they either increased
306 or decreased their activity following saccade onset. Accordingly, we classified these cells as
307 *facilitation* or *suppression* PCs, respectively (**Fig. 2**). The activity profile of the PCs was the same
308 during pro- and antisaccades in both areas, meaning that if one PC increased its firing rate after
309 saccade execution for prosaccades, it also increased it for antisaccades. This was true for all PCs
310 except for two in the lateral cerebellum, which showed a mixed firing behavior; these two cells
311 were included in their respective category for further analyses (e.g., as a *facilitation* cell in
312 prosaccade trials and a *suppression* cell in antisaccade trials).

313 We next assessed SS activity during the instruction period (for details, see **Methods**).
314 Given the variable duration of the instruction period, which ranged between 300 and 500 ms, we
315 analyzed the last 300 ms of this epoch, before target onset (**Fig. 1A**). Here, we also encountered
316 diverse neural responses in both regions. We classified the activity of these neurons in the same
317 way as for the saccade period, depending on whether they increased (*facilitation* PCs), or decreased
318 (*suppression* PCs) their SS firing during the instruction period compared to the activity during the
319 intertrial interval. The medial compared to the lateral cerebellum had overall less *facilitation* PCs
320 (Medial pro 10%, medial anti ~11%, Lateral pro ~17%, Lateral anti ~18%) and *suppression* PCs
321 (Medial pro ~11%, Medial anti ~7%, Lateral pro ~14%, Lateral anti ~15%) during the instruction
322 of pro- and antisaccade trials (**Fig. 2B-F**). The remaining cells had no change in firing rates during
323 the instruction period (medial: ~61%, lateral 36%).

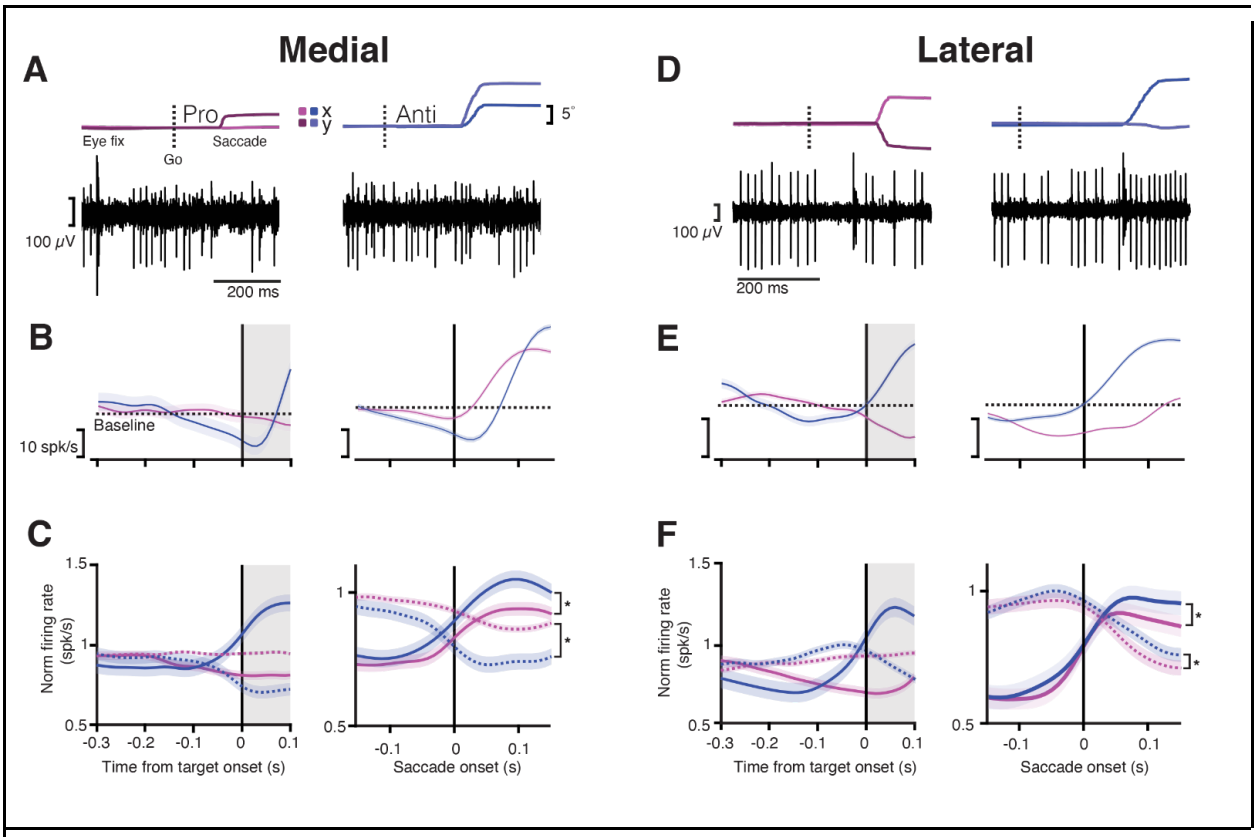

Figure 2. PCs in both medial and lateral cerebellum start modulating their activity during the instruction period. ***A top***, Eye trace for an example trial during saccade onset for a pro- (left) and antisaccade (right). Dashed line indicates the time of the "go" cue. Dark and light magenta and blue show the x and y position (horizontal and vertical components) of the eye trace for pro- and antisaccades respectively; ***bottom***, traces of activity recorded from a PC in medial cerebellum for a single trial aligned to the eye trace indicated above. Note that the traces include many simple spikes (SSs; smaller spikes) and only a few complex spikes (CSs, bigger spikes). ***B***, ***left*** Average response time-course for one example neuron aligned to the end of the instruction period (target onset) for prosaccades (magenta) and antisaccades (blue) for medial cerebellum. Dashed line shows the baseline mean. Shaded regions denote s.e.m. Gray shaded areas show time after the instruction period when the target appears, but the animals must keep fixating at the central dot; ***right*** Average response time-course for one example neuron aligned to saccade onset. Dashed line shows the baseline mean. **C,** Time-course of normalized responses averaged for all neurons in medial cerebellum that either increased their firing (*facilitation* cells, solid line) or decreased it (*suppression* cells, dashed lines) aligned to target onset (left) or saccade onset (right). Statistical comparisons after saccade onset, facilitation pro vs anti: $p = 1.61\text{x}10^{-7}$, suppression pro vs anti: $p = 5.3\text{x}10^{-23}$. ***D,*** Same as in (a) but for lateral cerebellum. ***E***, Same as in (b) but for lateral cerebellum. ***F***, Same as in (c) for lateral cerebellum (facilitation pro vs anti: $p = 1.08\text{x}10^{-17}$, suppression pro vs anti: $p = 4.4\text{x}10^{-9}$). Prosaccades are denoted in magenta and antisaccades in blue for all panels.

To relate PC activity during the instruction period with the subsequent saccade period, we next looked at the timing of the SS activity of *facilitation* and *suppression* PCs between medial and lateral cerebellum pooling the pro- and antisaccade conditions (**Fig. 2**). We found that the

327 latencies of the *suppression* PCs in the lateral cerebellum, measured at the trough after saccade
328 onset, were significantly longer than those in the medial cerebellum (mean ± s.d. Lateral 133 ± 40
329 ms vs. Medial 89 ± 68 ms, $p = 0.01$; Wilcoxon rank sum, **Fig. 2C** and **F**). In contrast, the *facilitation*
330 PCs showed similar timing of the peak activity in the medial and lateral cerebellum (mean ± s.d.
331 Medial 105 ± 41 ms vs. Lateral pro 84 ± 48 ms; $p = 0.4$; Wilcoxon rank sum). There were no
332 differences between prosaccades and antisaccades in this respect, neither for *suppression* PCs
333 (mean ± s.d. Medial pro 87 ± 70 ms vs. Medial anti 93 ± 67 ms, $p = 0.83$; Lateral pro 139 ± 40 ms
334 vs. Lateral anti 127 ± 42 s; $p = 0.1$; Wilcoxon Rank sum test), nor for *facilitation* PCs (mean ± s.d.
335 Medial pro 105 ± 41 ms vs. Medial anti 104 ± 33 ms, $p = 0.2$; Lateral pro 84 ± 48 ms vs. Lateral
336 anti 106 ± 43 ms, $p = 0.9$; Wilcoxon Rank sum test).

337 Together, these results suggest that PCs in the lateral cerebellum are more prominently
338 involved in the instruction of planned saccades than those in the medial cerebellum, and that the
339 course of SS responses of *suppression* PCs in the lateral cerebellum during the subsequent saccade
340 period is delayed with respect to that in the medial cerebellum.

341

342 *PCs in lateral cerebellum show a stronger modulation during the instruction period*

343 We observed that in some PCs the SS modulation ramped throughout the interval between
344 the instruction and the saccade epoch (**Fig. 2B-E** and **Fig. 3A**). We quantified the ramping of SS
345 activity by fitting a linear model to the firing rate during the last 300 ms of the instruction period,
346 and we classified PCs as ramping cells when R^2 was higher than 0.75. We found that ramping
347 modulation was quite rare in the medial cerebellum and more prevalent in the lateral cerebellum
348 (**Fig. 3B**); this held true for both prosaccade and antisaccade trials (Medial n (pro) = 3, n (anti) =

349 2; Lateral n (pro) = 11, n (anti) = 10; both comparisons $p = 0.02$; χ^2 test). Overall, we found more

350 PCs that significantly changed their firing from baseline during the instruction period in the lateral

351 cerebellum than in the medial cerebellum (Medial vs Lateral, $p = 0.03$; Mann-Whitney test),

352 suggesting a more prominent role for PC modulation in the lateral cerebellum during instruction.

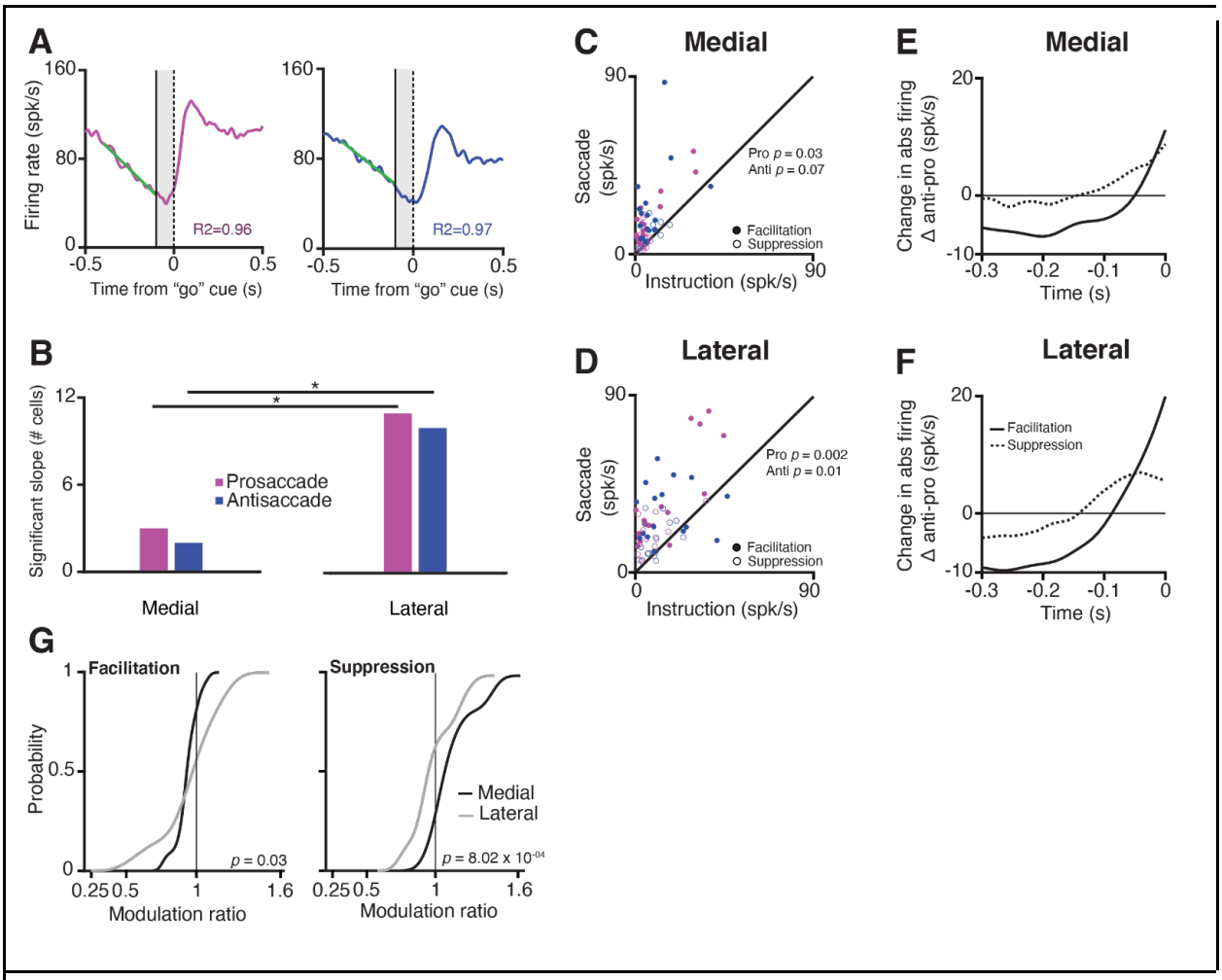

Figure 3. PCs in the lateral cerebellum exhibit stronger modulation than PCs in the medial cerebellum during the instruction period. ***A*****,** Explanation of slope calculations used for panel (b); ***left***, Time-course of responses during prosaccades (magenta) and antisaccades (blue) for an example neuron in the lateral cerebellum aligned to "go" cue (vertical dashed line at zero); *right*, activity of the same neuron, but now for an antisaccade trial also aligned to the "go" cue . Solid vertical line shows the end of the instruction period, shaded area is when the target appears but the NHPs must keep fixating. A linear regression model was fitted (orange diagonal solid and green dotted line, for pro- and antisaccades, respectively) to the firing rate 300 ms before the end of the instruction period to calculate the slopes (see **Methods**). ***B*****,** Number of cells with significant slope modulation in the medial and lateral cerebellum ($\chi 2$ test for proportions) during pro- and antisaccades ($p = 0.02$ for both comparisons). ***C*****,** Scatter plots of maximum simple spike firing rate change of PCs during the instruction period vs. that during the saccade

period (in spks/s) for pro- and antisaccades in medial cerebellum. ***D***, Same as in (c) but for lateral cerebellum. ***E***, Difference in change in absolute firing rate between pro- and antisaccades (abs antisaccade SS activity- abs prosaccade SS activity) for *facilitation* and *suppression* neurons in medial cerebellum. ***F*,** Same as in (e) but for lateral cerebellum. ***G***, Cumulative distribution of the SS modulation ratio for medial and lateral cerebellum for *facilitation* and *suppressive* PCs. Insets show *p*-values for the comparison between medial and lateral cerebellum (two sample K-S test).

When we investigated the changes in the firing rate (modulation, **Methods**) for each PC during the instruction and saccade period within the medial and lateral cerebellum, we found that in the lateral cerebellum, the maximum change in the firing rate was significantly lower during the instruction period than during the saccade period, for both pro- and antisaccade trials (Lateral pro $p = 0.002$, anti $p = 0.01$; Wilcoxon rank sum test) (**Fig. 3C**). In the medial cerebellum only the prosaccade trails showed this trend (Medial pro $p = 0.03$, anti $p = 0.07$, Wilcoxon rank sum test) (**Fig. 3D**).

Further examination of the differences in responses during pro- and antisaccades showed that *facilitation* and *suppression* cells in the lateral cerebellum show significant encoding of SS modulation for trial conditions. We calculated a modulation ratio between the responses during the saccade period in the two types of trials, defined as the ratio between the response during pro- and antisaccades (**Fig. 3G**, **Methods**). Values of 1 indicate that both responses are the same, values higher than 1 indicate that prosaccade activity was higher, and below 1 that antisaccade activity was higher. Medial PCs had somewhat different responses when comparing pro- and antisaccade activity in contrast to lateral PCs (mean of *facilitation* PCs in medial cerebellum 0.91 ± 0.1 s.d. versus that in lateral cerebellum 0.88 ± 0.3, $p = 0.03$; mean of *suppression* PCs in medial cerebellum 1.16 ± 0.2 versus that in lateral cerebellum 1 ± 0.2, $p = 8.02 \times 10^{-04}$; one-tailed K-S test). To summarize, PCs in both medial and lateral cerebellum modulate their activity during

372 instruction of pro- and antisaccades, with a relatively bigger role for the *facilitation* cells during
373 the instruction of antisaccades. Yet, PCs in the lateral cerebellum differ from those in the medial
374 cerebellum in that they have a relatively stronger modulation in both the instruction and saccade
375 periods as well as for the pro- vs antisaccade conditions.

376

377 *Differences between facilitation and suppression cells that occur in both medial and lateral*
378 *cerebellum*

379 In addition to the observed differences across the recorded regions, we identified features
380 that were shared across the medial and lateral cerebellum. First, we observed that *facilitation* and
381 *suppression* PCs in medial and the lateral cerebellum operate at different baseline frequencies,
382 which is in line with the upbound and downbound modules of PCs described for the cerebellar
383 cortex of rodents (De Zeeuw, 2021). Since these modules have been hypothesized to operate at a
384 relatively low and high baseline SS firing frequency, respectively, so as to leave ample room for
385 increases and decreases during epochs of stimulation and modulation, we investigated whether the
386 *suppression* and *facilitation* cells differed in this respect (see also (Sun et al., 2017; Herzfeld et al.,
387 2018; Soetedjo et al., 2019). We found that *suppression* cells started at a relatively high baseline
388 SS firing frequency in both the medial and lateral cerebellum (62.43 ± 3.76 spks/s and 69.6 ± 6.12
389 spks/s, respectively), and *facilitation* cells started at a significantly lower baseline SS firing
390 frequency in both regions (56.36 ± 3.65 spks/s and 54.72 ± 3.76 spks/s, p = 0.02; one-tailed
391 Wilcoxon rank-sum test comparison between all *facilitation* vs *suppression* cells pooled in both
392 areas).

393 Next, we found that whereas the saccade period contained more *suppression* PCs, during
394 the instruction period the contribution of the *facilitation* cells appeared most prominent,
395 particularly during that of the antisaccade trials. When we subtracted the SS modulation during
396 the prosaccade trails from the activity during the antisaccade trials (antisaccade SS activity -
397 prosaccade SS activity), *facilitation* PCs in both medial and lateral cerebellum showed a larger
398 change in firing rate just before the target onset during the instruction period (**Fig. 3E, F**). These
399 changes were significantly less pronounced for *suppression* cells (*facilitation* PCs versus
400 *suppression* PCs in medial cerebellum p = 4.4x10-6; *facilitation* PCs versus *suppression* PCs in
401 lateral cerebellum p = 0.004; Wilcoxon Rank sum test). Thus, *facilitation* and *suppression* cells
402 can be characterized by several features that are common for medial and lateral cerebellum.

403

404 *The lateral but not the medial cerebellum contains information about stimulus identity during the*
405 *instruction period*

406 To extract the features of the population activity related to pro- and antisaccades we applied
407 a linear dimensionality reduction technique: demixed principal component analysis (dPCA,
408 (Kobak et al., 2016). dPCA demixes the neural activity into activity related to the task components
409 that capture the most variance in the data. The dPCA was used to investigate to what extent the
410 neurons are tuned to two stimulus conditions indicated by the color of the fixation point (i.e. the
411 pro- or antisaccades), or whether their activity is condition-independent. In the condition-
412 independent group, dPCA components show task related activity modulations that cannot be
413 assigned to one of the stimulus conditions. As explained above, due to the high behavioral
414 performance of both NHPs, our dataset lacked the power to create another category with decision-
415 related components in correct/incorrect trials. dPCA was applied to the entire population of

416 recorded cells in the medial (n = 90) and the lateral cerebellum (n = 72). We included cells which
417 had at least 5 trials in pro- and antisaccade conditions. The results were cross-validated to measure
418 time-dependent classification accuracy and a shuffling procedure was applied to assess whether
419 classification accuracy was significantly above chance level (see **Methods**).

420 In the medial cerebellum, the overall variance explained by the dPCA components was
421 mostly captured by the first 3 components, which were independent of the stimulus condition, and
422 together they explained 66.9 % of variance, (**Fig. 4A**). These components all have strong activity
423 after the end of the instruction, and thus around the time the animal initiates the saccade (**Fig. 4B**).
424 Components 4, 5 and 7 were selected as containing the strongest activity differences in relation to
425 the stimulus conditions (**Fig. 4B**, bottom row and **Fig. 4C**). To determine significance, each
426 component was used as a linear decoder to classify each of the stimulus conditions (see **Methods**).
427 No components could reliably be used to classify the stimulus condition in the medial cerebellum.

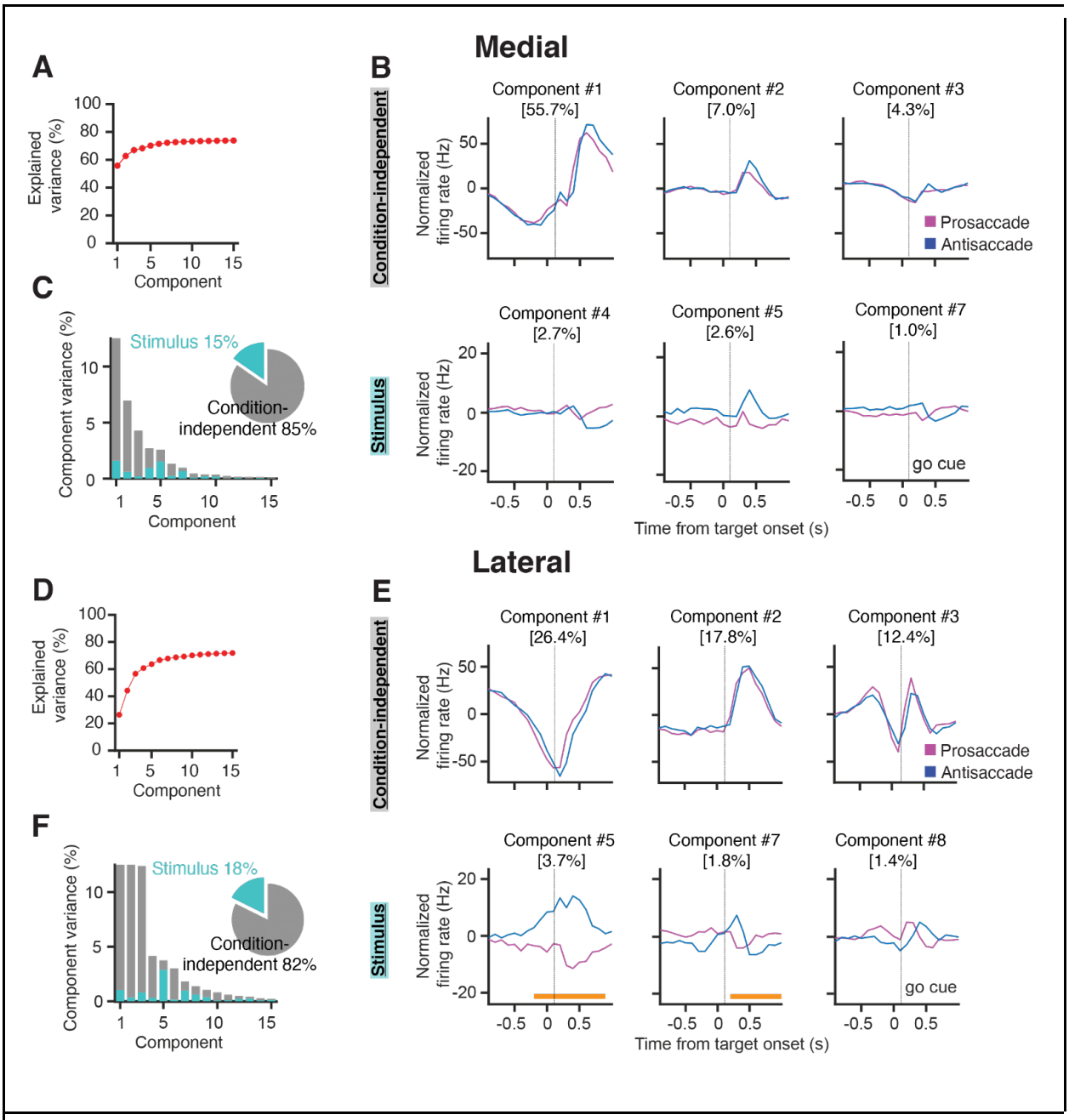

Figure 4. Demixed PCA indicates that PCs in the lateral cerebellum encode stimulus identity. *A*, Cumulative fraction of variance explained by dPCA in the medial cerebellum. Dotted line indicates an estimate of the fraction of variance in the data explained by the dPCA. ***B*,** Projections of the PSTH's of all medial cerebellar PCs onto the most prominent decoding axes; ***top***, first three condition-independent components; ***bottom***, first three stimulus-related (pro/anti) components. Percentages denote variance captured by each component. Time from instruction offset. ***C***, Variance of the individual demixed principal components for the medial cerebellum. Each bar shows the proportion of total variance. Gray bars depict condition-independent variance, cyan bars indicate stimulus-related (pro/anti) variance. Pie chart shows the total signal variance for stimulus-related and condition-independent components. ***D-F***, Same as in (A-C) but for the lateral cerebellum, orange horizontal bars in ***E*** indicate time during which the stimulus can be decoded from the population firing rate.

428

429 Similar to the medial cerebellum, components 1, 2 and 3 of the lateral cerebellum captured
430 most of the variance in the condition independent categories (56.4%, **Fig 4E**). These components
431 also showed a strong modulation after instruction offset. In contrast to the medial cerebellum, two
432 of these components modulated during most of the instruction period (**Fig. 4F).** Stimulus related
433 components showed significant tuning for pro- and/or antisaccades in components 5 and 7.
434 Notably, in component 5, stimulus condition classification was already possible almost 200 ms
435 before the end of the instruction period. In the lateral cerebellum the variance in this component
436 could almost be entirely attributed to the stimulus conditions (**Fig. 4F**). Indeed, in component 5,
437 the time period in which the stimulus condition could be decoded from the firing rates was broad,
438 bridging the instruction period to the saccade. This appears to be in line with the prominent
439 ramping modulation described in **Figure 3**. These results show that PCs in the lateral, but not in
440 the medial, cerebellum contain reliable information about the trial identity during the instruction
441 period.

442

443 *Complex spike responses of PCs in the lateral cerebellum show reciprocal activity with simple*
444 *spike responses*

445 In a subset of recorded PCs, we were able to reliably isolate and analyze CS responses
446 throughout all trials. We restricted the CS analysis only to cells with average CS firing rates higher
447 than 0.5 Hz over the duration of the whole recording (Medial n = 11, Lateral n = 18). Similar to
448 the SS analyses, we examined the CS responses separately in the medial and lateral cerebellum
449 during the instruction and saccade periods (**Fig. 5**). The average CS activities during the instruction

450 (1.10 Hz ± 0.47 s.d., n = 11) and saccade (1.11 Hz ± 0.50 s.d., n = 11) period in the medial
451 cerebellum were not significantly different from those in the lateral cerebellum (1.15 Hz ± 0.33
452 s.d., n = 18 and 1.13 Hz ± 0.52 s.d., n = 18, respectively; $p = 0.87$ and $p = 0.36$ for comparison
453 medial versus lateral during instruction and saccade period, respectively; Wilcoxon rank sum).

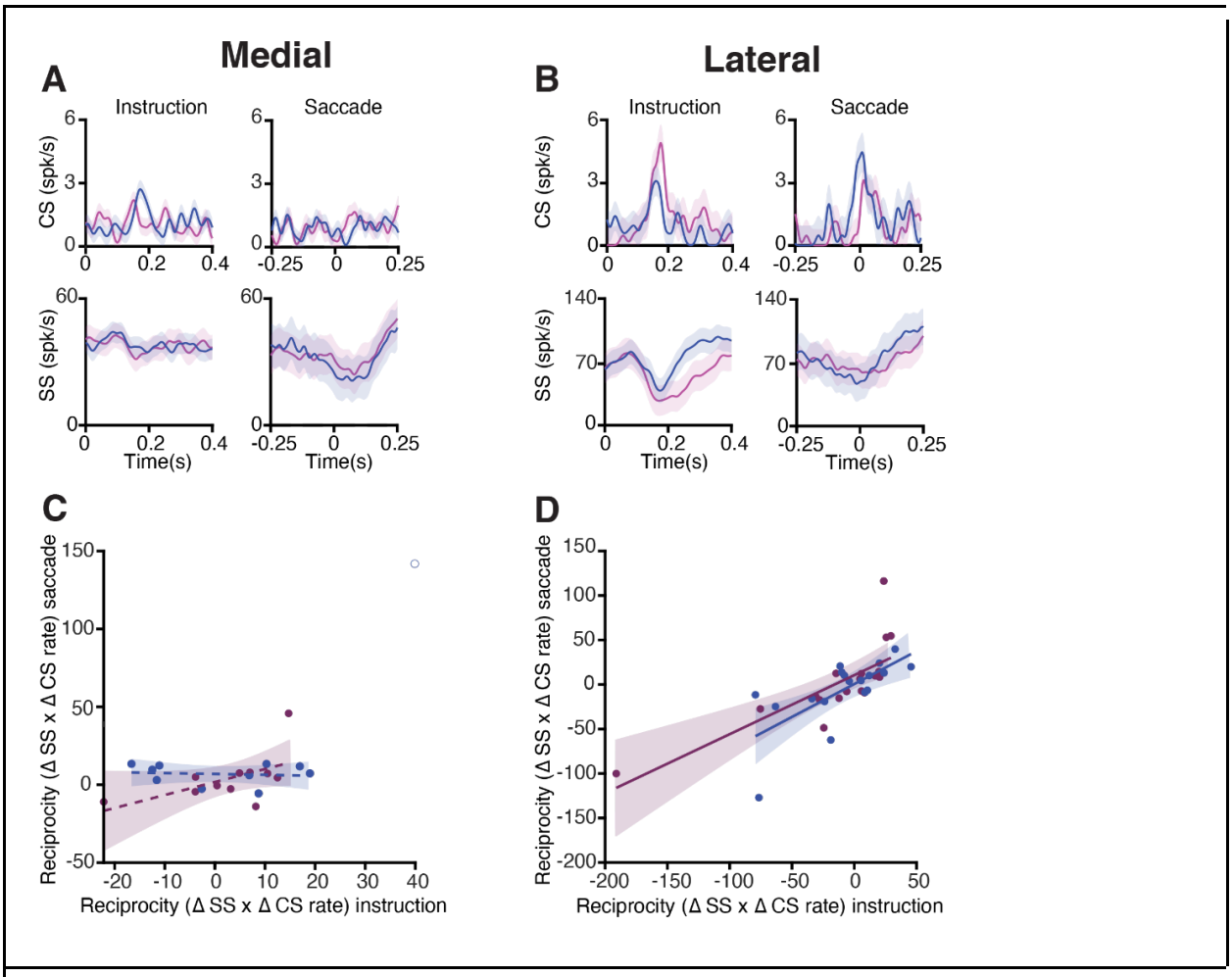

Figure 5. Complex spike and simple spike interaction during pro- and antisaccade trials. ***A***, Top, average CS rate of PCs in medial cerebellum during prosaccades (magenta) and antisaccades (blue) aligned to the onset of the instruction (left) and saccade (right) period. Bottom panels show the associated SS responses. Shaded areas represent s.e.m. ***B***, Same as *A*, but for neurons recorded in the lateral cerebellum. ***C***, Relation of reciprocity between CS and SS responses during instruction and saccade period. To quantify the reciprocity, we calculated the maximum change in CS firing rate in the windows of interest (instruction and saccade period), the associated maximum change in SS rate in a window of 300 ms around the peak of CS activity, and subsequently the product of the two (Δ CS rate x Δ SS rate). Note that if a positive modulation of CSs is associated with a negative modulation of SSs, the reciprocity measure presented here will give a negative value. If CSs and SSs show simultaneous positive modulations, and thus no reciprocity, this will result in a positive value. Every dot represents one cell.

One outlier was removed from the medial antisaccade group (unfilled blue dot). The coefficients of determination (R^2) are: medial pro 0.30, medial anti 0.01. **D**, same as C but of lateral neurons, coefficients of determination: lateral pro 0.59, and lateral anti 0.48. Shading indicates 95% confidence interval of the regression lines.

Next, we quantified the interaction between CS and SS responses during the instruction period (**Fig. 5A** and **B,** left panels). For every PC of both medial and lateral cerebellum we calculated the maximum change in CS firing rate from the baseline in the instruction window and the maximum change in SS firing rate from baseline in the 300 ms window around the time of the peak CS rate. This was also done for the saccade period for the pro- and antisaccade trials separately. Change in CS firing from the baseline was multiplied with change in SS firing from baseline to establish their interdependence, i.e., reciprocity (Badura et al., 2013). To determine whether reciprocity was dependent on both epochs, linear regression was applied on the reciprocity values in the instruction and saccade windows (**Fig 5C, D)**. Lateral cerebellar PCs had a positive association with reciprocity during the instruction and the saccade period, whereas medial cerebellum did not (coefficients of determination (R^2) : lateral pro 0.59, and lateral anti 0.48, medial pro 0.30, medial anti 0.01).

Discussion

The antisaccade task has been used to investigate flexible behavioral control, where a correct suppression of a prosaccade followed by a response to the opposite direction forms a feature of executive control (Mokler and Fischer, 1999; Mitchell et al., 2002). We found evidence for cerebellar involvement in volitional control of this behavior in both medial (i.e., OMV) and lateral (i.e., crus I/II) cerebellar cortex by recording the activity of PCs during pro- and antisaccades in NHPs. Our findings add to the growing body of evidence pointing to an important contribution of the cerebellum to cognitive processes in general and particularly voluntary behavior. We demonstrated that PCs in both areas modulate their activity depending on the trial type, and that SS responses of populations of PCs in the lateral cerebellum are able to discriminate the type of trial before the eye movement takes place. Even though the lateral cerebellum is not traditionally viewed as a saccade-control area, our findings support early reports where saccades are elicited following electrical stimulation to lateral regions of the hemispheres, especially in crus I/II (Ron and Robinson, 1973).

Antisaccades exhibit kinematic properties that differ from prosaccades, a result consistent with previous reports in human and non-human primates (Amador et al., 1998; Munoz and Everling, 2004). Even so, the preferential modulations of SS responses in the PCs were not correlated to any of those kinematic changes. This suggests that the observed activity was not merely an efference copy of the motor command but may also reflect the preparatory or planning phase of the voluntary movement in which the PC firing is determined by the cue. This is in line with recent findings in cerebellar atrophy patients who show impairments when making goal-oriented movements (Piu et al., 2019).

489 Various parameters of PC activity differed between medial and lateral cerebellum. SS
490 activity of PCs in the lateral cerebellum (1) displayed more signal separation/selectivity for pro-
491 and antisaccades during the instruction period, suggesting that the population contains information
492 about the trial identity, (2) showed a greater firing rate during the execution of saccades. Likewise,
493 their CS activity showed a higher level of reciprocity with respect to simple spike activity, during
494 both the instruction and execution period. Together, these data indicate that different modules of
495 different cerebellar regions can contribute to the same complex behavior, yet with different
496 propensities.

497 *PC modulation during instruction period*

498 Studies from cerebellar patients suggest that the cerebellum might not be involved in the
499 initiation of saccades, but in the correct and accurate execution of them (Kornhuber, 1971; Thier
500 et al., 2002). Our results indicate that PCs in the lateral cerebellum encode information about the
501 trial identity. The dPCA analysis in Crus I/II PCs exhibited significantly different SS activity
502 between both conditions, showing that these contain sufficient information to distinguish a pro-
503 from an antisaccade. This is supported by a previous study showing that downstream neurons in
504 the dentate nucleus modulate during preparation of antisaccades and that inactivation thereof
505 promotes antisaccade errors (Kunimatsu et al., 2016). This instruction-related activity in
506 antisaccade trials may be relayed to brainstem nuclei that are engaged in curtailing reflexive
507 saccades (Everling et al., 1999). The persistent SS modulation of PCs in lateral cerebellum upon
508 cue presentation suggests that it updates an internal model for well-timed activity during motor
509 planning, which may be relayed to the prefrontal cortex (Gao et al., 2018).

510 Correct decoding of a visual stimulus is an essential component of the pro- and antisaccade
511 task. Visual responses in the cerebellum have been reported in several areas including the floccular

512 complex, crus I/II and the inferior semilunar lobe (VII/VIII) (Marple-Horvat and Stein, 1990).
513 Dentate nucleus neurons have activity bridging the period from task instructions to motor
514 execution (Kunimatsu et al., 2016), which could be derived from the same population of PC's as
515 we recorded in the lateral cerebellum. Our results on the relatively prominent CS - SS reciprocity
516 in lateral cerebellum raise the possibility that CS responses play a similar role in decoding visual
517 stimuli for the preparation of ensuing movements.

518 Contemporary models of antisaccade decision-making require evidence accumulation to
519 reach a decision boundary in the frontal cortex (Munoz and Everling, 2004). PCs receive diverse
520 sensory, motor and cognitive information through their parallel fiber inputs, which may facilitate
521 efficient evidence accumulation. Classical models of cerebellar function indicate that climbing
522 fiber mediated plasticity in the molecular layer determines which parallel fiber inputs are turned
523 into SS modulation (Gao et al., 2012). The PCs that we measured in the lateral cerebellum carry
524 both SS and CS signals during the instruction period of the antisaccade task. We hypothesize that
525 through the pre-learned associations of parallel fiber and climbing fiber signals, relevant evidence
526 from the stimulus (i.e., dot color in instruction) for the selection of the required action (i.e., pro-
527 or antisaccade) can be rapidly relayed from the lateral cerebellum to the frontal saccade areas. In
528 cerebellar patients, latencies for antisaccades are prolonged, indicating a less efficient decision-
529 making process in absence of cerebellar input (Piu et al., 2019).

530 *PC modulation during saccade execution*

531 Single PCs modulated their SS activity during the execution of pro- and antisaccades in
532 both medial and lateral cerebellum, but only lateral PCs were able to successfully discriminate the
533 type of trial. Despite the heterogeneity of the responses, neurons that facilitated or suppressed their
534 response after saccade onset exhibited differential activity during pro- and antisaccade trials (**Fig.**

535 **3**). As a population, PC responses were different when executing a saccade towards a visible target
536 than when using an internally generated goal. This is particularly interesting for two reasons: First,
537 medial cerebellum has always been identified as a motor and timing controller for the different
538 types of saccades, interacting with cortical and brainstem brain areas (McElligott and Keller, 1984;
539 Noda and Fujikado, 1987; Thier and Möck, 2006; Herzfeld et al., 2015, 2018), while the role of
540 the lateral cerebellum in saccade control has remained under debate. Indeed, lesions of lateral
541 cerebellum can delay onset of saccades between 10 and 60 ms and result in variable hypo- and
542 hypermetria (Ohki et al., 2009), but the contribution of Purkinje cell activity in the lateral
543 cerebellum to proactive control of saccades and flexible behavioral in general has not been
544 conclusively proven. Second, differential cerebellar activity during antisaccades implies that it
545 contains neural signatures to modulate preparation and execution by encoding information about
546 the current context of the upcoming action (saccade), which is necessary for the fast classification
547 of the response as correct or erroneous. This finding is in line with the impact of focal cerebellar
548 lesions in humans on the changes in potentials observed during performance monitoring in an
549 antisaccade task (Peterburs et al., 2012).

550 *Cerebellar modules operate in parallel*

551 The data on *suppression* PCs in the medial cerebellum showing a relatively early SS
552 modulation during execution of both pro- and antisaccades as well as those on *facilitation* PCs in
553 the lateral cerebellum showing a prominent modulation at the end of the instruction of antisaccades
554 indicate that different modules of different cerebellar regions can simultaneously contribute to the
555 same complex behavior, yet with different particularities. A similar conclusion was drawn from a
556 recent study on delay eyeblink conditioning (Wang et al., 2020). Even though this form of
557 conditioning is classically considered to be controlled solely by modules in lobule simplex of the

558 lateral cerebellum, Wang and colleagues have shown that modules of the medial cerebellum are
559 equally essential, yet also contributing in a slightly differential fashion, possibly regulating mainly
560 muscle tone. Similar to the current pro- and antisaccade tasks, during eyeblink conditioning the
561 medial and lateral cerebellum also both engage *facilitation (i.e., upbound)* and *suppression (i.e.,*
562 *downbound)* cells, and they also operate at relatively low and high baseline firing frequencies,
563 respectively (ten Brinke et al., 2015; Wang et al., 2020). Our current finding that *facilitation* and
564 *suppression* cells appear to play a more dominant role during the instruction and execution of the
565 saccade task, respectively, further highlights the differential functional relevance of the upbound
566 and downbound modules (De Zeeuw, 2021).

567 Previous reports of activity in the dentate nucleus, which is the main target of PCs in the
568 lateral cerebellum, have shown mixed evidence regarding the direction of modulation during
569 saccade-related behavior (Ashmore and Sommer, 2013; Kunimatsu et al., 2018). Kunimatsu and
570 colleagues (2018) found only upward modulating units during self-initiated saccades, whereas
571 Ashmore and Sommer (2013) revealed groups of both facilitating and suppressing cells during
572 delayed saccades. Possibly, these differences reflect differences in the behavioral paradigms and/or
573 downstream pathways involved (De Zeeuw, 2021). In our dataset, the modulation exhibited by
574 PCs is bidirectional in both medial and lateral cerebellum with populations of both *facilitation* and
575 *suppression* cells.

576

577

578

579

580 **References**

581 Amador N, Schlag-Rey M, Schlag J (1998) Primate antisaccades. I. Behavioral
582 characteristics. J Neurophysiol 80:1775–1786.

583 Ashmore RC, Sommer MA (2013) Delay activity of saccade-related neurons in the caudal
584 dentate nucleus of the macaque cerebellum. J Neurophysiol 109:2129–2144.

585 Badura A, Schonewille M, Voges K, Galliano E, Renier N, Gao Z, Witter L, Hoebeek FE,
586 Chedotal A, De Zeeuw CI (2013) Climbing fiber input shapes reciprocity of Purkinje cell
587 firing. Neuron 78:700–713.

588 Brunamonti E, Chiricozzi FR, Clausi S, Olivito G, Giusti MA, Molinari M, Ferraina S,
589 Leggio M (2014) Cerebellar damage impairs executive control and monitoring of
590 movement generation. PLoS One 9:e85997.

591 Bunge SA, Wallis JD, Parker A, Brass M, Crone EA, Hoshi E, Sakai K (2005) Neural
592 circuitry underlying rule use in humans and nonhuman primates. J Neurosci 25:10347–
593 10350.

594 Caligiore D, Pezzulo G, Baldassarre G, Bostan AC, Strick PL, Doya K, Helmich RC, Dirkx
595 M, Houk J, Jorntell H, Lago-Rodriguez A, Galea JM, Miall RC, Popa T, Kishore A,
596 Verschure PF, Zucca R, Herreros I (2017) Consensus Paper: Towards a Systems-Level
597 View of Cerebellar Function: the Interplay Between Cerebellum, Basal Ganglia, and
598 Cortex. Cerebellum 16:203–229.

599 Chabrol FP, Blot A, Mrsic-Flogel TD (2019) Cerebellar Contribution to Preparatory

Activity in Motor Neocortex. Neuron 103:506–519.e4.

Coe BC, Munoz DP (2017) Mechanisms of saccade suppression revealed in the anti-saccade task. Philos Trans R Soc Lond B Biol Sci 372 Available at: http://dx.doi.org/10.1098/rstb.2016.0192.

Cutsuridis V, Kumari V, Ettinger U (2014) Antisaccade performance in schizophrenia: a neural model of decision making in the superior colliculus. Front Neurosci 8:13.

Dacre J, Colligan M, Ammer J, Schiemann J, Clarke T, Chamosa-Pino V, Claudi F, Alex Harston J, Eleftheriou C, Pakan JMP, Huang C-C, Hantman A, Rochefort NL, Duguid I (2019) Cerebellar-recipient motor thalamus drives behavioral context-specific movement initiation. bioRxiv:802124 Available at: https://www.biorxiv.org/content/10.1101/802124v1 [Accessed October 23, 2019].

De Schutter E (2019) Fallacies of Mice Experiments. Neuroinformatics 17:181–183.

Deverett B, Koay SA, Oostland M, Wang SS-H (2018) Cerebellar involvement in an evidence-accumulation decision-making task. Elife 7 Available at: http://dx.doi.org/10.7554/eLife.36781.

De Zeeuw CI (2021) Bidirectional learning in upbound and downbound microzones of the cerebellum. Nat Rev Neurosci 22:92–110.

Diamond A (2013) Executive functions. Annu Rev Psychol 64:135–168.

Everling S, Dorris MC, Munoz DP (1999) Neuronal Activity in Monkey Superior Colliculus during an Antisaccade Task. In: Current Oculomotor Research: Physiological

620 and Psychological Aspects (Becker W, Deubel H, Mergner T, eds), pp 17–23. Boston, MA:
621 Springer US.

622 Everling S, Fischer B (1998) The antisaccade: a review of basic research and clinical
623 studies. Neuropsychologia 36:885–899.

624 Everling S, Johnston K (2013) Control of the superior colliculus by the lateral prefrontal
625 cortex. Philos Trans R Soc Lond B Biol Sci 368:20130068.

626 Funahashi S, Chafee MV, Goldman-Rakic PS (1993) Prefrontal neuronal activity in rhesus
627 monkeys performing a delayed anti-saccade task. Nature 365:753–756.

628 Gao Z, Davis C, Thomas AM, Economo MN, Abrego AM, Svoboda K, De Zeeuw CI, Li N
629 (2018) A cortico-cerebellar loop for motor planning. Nature 563:113–116.

630 Gao Z, Thomas AM, Economo MN, Abrego AM, Svoboda K, De Zeeuw CI, Li N (2019)
631 Response to "Fallacies of Mice Experiments." Neuroinformatics 17:475–478 Available at:
632 http://dx.doi.org/10.1007/s12021-019-09433-y.

633 Gao Z, van Beugen BJ, De Zeeuw CI (2012) Distributed synergistic plasticity and
634 cerebellar learning. Nat Rev Neurosci 13:619–635.

635 Giovannucci A, Badura A, Deverett B, Najafi F, Pereira TD, Gao Z, Ozden I, Kloth AD,
636 Pnevmatikakis E, Paninski L, De Zeeuw CI, Medina JF, Wang SS (2017) Cerebellar
637 granule cells acquire a widespread predictive feedback signal during motor learning. Nat
638 Neurosci 20:727–734.

639 Goldring J, Fischer B (1997) Reaction times of vertical prosaccades and antisaccades in gap

640 and overlap tasks. Exp Brain Res 113:88–103.

641 Gottlieb J, Goldberg ME (1999) Activity of neurons in the lateral intraparietal area of the
642 monkey during an antisaccade task. Nat Neurosci 2:906–912.

643 Hakvoort Schwerdtfeger RM, Alahyane N, Brien DC, Coe BC, Stroman PW, Munoz DP
644 (2012) Preparatory neural networks are impaired in adults with attention-
645 deficit/hyperactivity disorder during the antisaccade task. Neuroimage Clin 2:63–78.

646 Herzfeld DJ, Kojima Y, Soetedjo R, Shadmehr R (2015) Encoding of action by the Purkinje
647 cells of the cerebellum. Nature 526:439–442.

648 Herzfeld DJ, Kojima Y, Soetedjo R, Shadmehr R (2018) Encoding of error and learning to
649 correct that error by the Purkinje cells of the cerebellum. Nat Neurosci 21:736–743.

650 Ito M (2008) Control of mental activities by internal models in the cerebellum. Nat Rev
651 Neurosci 9:304–313.

652 Kelly RM, Strick PL (2003) Cerebellar loops with motor cortex and prefrontal cortex of a
653 nonhuman primate. J Neurosci 23:8432–8444.

654 Kobak D, Brendel W, Constantinidis C, Feierstein CE, Kepecs A, Mainen ZF, Qi X-L,
655 Romo R, Uchida N, Machens CK (2016) Demixed principal component analysis of neural
656 population data. Elife 5 Available at: http://dx.doi.org/10.7554/eLife.10989.

657 Kornhuber HH (1971) Motor functions of cerebellum and basal ganglia: the
658 cerebellocortical saccadic (ballistic) clock, the cerebellonuclear hold regulator, and the basal
659 ganglia ramp (voluntary speed smooth movement) generator. Kybernetik 8:157–162.

660 Kostadinov D, Beau M, Pozo MB, Häusser M (2019) Predictive and reactive reward signals
661 conveyed by climbing fiber inputs to cerebellar Purkinje cells. Nat Neurosci 22:950–962.

662 Kunimatsu J, Suzuki TW, Ohmae S, Tanaka M (2018) Different contributions of
663 preparatory activity in the basal ganglia and cerebellum for self-timing. Elife 7 Available at:
664 http://dx.doi.org/10.7554/eLife.35676.

665 Kunimatsu J, Suzuki TW, Tanaka M (2016) Implications of Lateral Cerebellum in Proactive
666 Control of Saccades. Journal of Neuroscience 36:7066–7074.

667 Marple-Horvat DE, Stein JF (1990) Neuronal activity in the lateral cerebellum of trained
668 monkeys, related to visual stimuli or to eye movements. J Physiol 428:595–614.

669 McElligott JG, Keller EL (1984) Cerebellar vermis involvement in monkey saccadic eye
670 movements: microstimulation. Exp Neurol 86:543–558.

671 Miall RC, Weir DJ, Wolpert DM, Stein JF (1993) Is the cerebellum a smith predictor? J
672 Mot Behav 25:203–216.

673 Mitchell JP, Macrae CN, Gilchrist ID (2002) Working memory and the suppression of
674 reflexive saccades. J Cogn Neurosci 14:95–103.

675 Mokler A, Fischer B (1999) The recognition and correction of involuntary prosaccades in
676 an antisaccade task. Exp Brain Res 125:511–516.

677 Munoz DP, Everling S (2004) Look away: the anti-saccade task and the voluntary control of
678 eye movement. Nat Rev Neurosci 5:218–228.

679 Noda H, Fujikado T (1987) Involvement of Purkinje cells in evoking saccadic eye

movements by microstimulation of the posterior cerebellar vermis of monkeys. J Neurophysiol 57:1247–1261.

Ohki M, Kitazawa H, Hiramatsu T, Kaga K, Kitamura T, Yamada J, Nagao S (2009) Role of primate cerebellar hemisphere in voluntary eye movement control revealed by lesion effects. J Neurophysiol 101:934–947.

Peterburs J, Gajda K, Koch B, Schwarz M, Hoffmann K-P, Daum I, Bellebaum C (2012) Cerebellar lesions alter performance monitoring on the antisaccade task--an event-related potentials study. Neuropsychologia 50:379–389.

Piu P, Pretegiani E, Rosini F, Serchi V, Zaino D, Chiantini T, Rufa A (2019) The cerebellum improves the precision of antisaccades by a latency-duration trade-off. Prog Brain Res 249:125–139.

Ron S, Robinson DA (1973) Eye movements evoked by cerebellar stimulation in the alert monkey. J Neurophysiol 36:1004–1022.

Schlag-Rey M, Amador N, Sanchez H, Schlag J (1997) Antisaccade performance predicted by neuronal activity in the supplementary eye field. Nature 390:398–401.

Sendhilnathan N, Semework M, Goldberg ME, Ipata AE (2020) Neural Correlates of Reinforcement Learning in Mid-lateral Cerebellum. Neuron 106:188–198.e5.

Soetedjo R, Kojima Y, Fuchs AF (2019) How cerebellar motor learning keeps saccades accurate. J Neurophysiol 121:2153–2162.

Strick PL, Dum RP, Fiez JA (2009) Cerebellum and nonmotor function. Annu Rev

Neurosci 32:413–434.

Sun Z, Smilgin A, Junker M, Dicke PW, Thier P (2017) The same oculomotor vermal Purkinje cells encode the different kinematics of saccades and of smooth pursuit eye movements. Sci Rep 7:40613.

Tanaka H, Harada M, Arai M, Hirata K (2003) Cognitive dysfunction in cortical cerebellar atrophy correlates with impairment of the inhibitory system. Neuropsychobiology 47:206–211.

ten Brinke MM, Boele HJ, Spanke JK, Potters JW, Kornysheva K, Wulff P, Ac IJ, Koekkoek SK, De Zeeuw CI (2015) Evolving Models of Pavlovian Conditioning: Cerebellar Cortical Dynamics in Awake Behaving Mice. Cell Rep 13:1977–1988.

Thach WT (2007) On the mechanism of cerebellar contributions to cognition. Cerebellum 6:163–167.

Thier P, Dicke PW, Haas R, Thielert C-D, Catz N (2002) The role of the oculomotor vermis in the control of saccadic eye movements. Ann N Y Acad Sci 978:50–62.

Thier P, Möck M (2006) The oculomotor role of the pontine nuclei and the nucleus reticularis tegmenti pontis. Prog Brain Res 151:293–320.

Voogd J, Schraa-Tam CK, van der Geest JN, De Zeeuw CI (2012) Visuomotor cerebellum in human and nonhuman primates. Cerebellum 11:392–410.

Wang X, Yu S-Y, Ren Z, De Zeeuw CI, Gao Z (2020) A FN-MdV pathway and its role in cerebellar multimodular control of sensorimotor behavior. Nat Commun 11:6050.

720 **Author contributions**

721 CIDZ, AB, MF, NF and EA designed the study and analysis. EA and PR performed surgeries on
722 the animals. EA and NF executed the experiments and EA, NF, AB and PJH analyzed the data.
723 EA, NF, AB and CIDZ wrote the first draft. All authors edited the manuscript.

724 **Data and code availability**

725 The data that support the findings of this study and code for analysis of in vivo eye movement and
726 Purkinje cell recordings are available from the corresponding author upon reasonable request.